Volume 11 | Number 22 | 21 November 2024

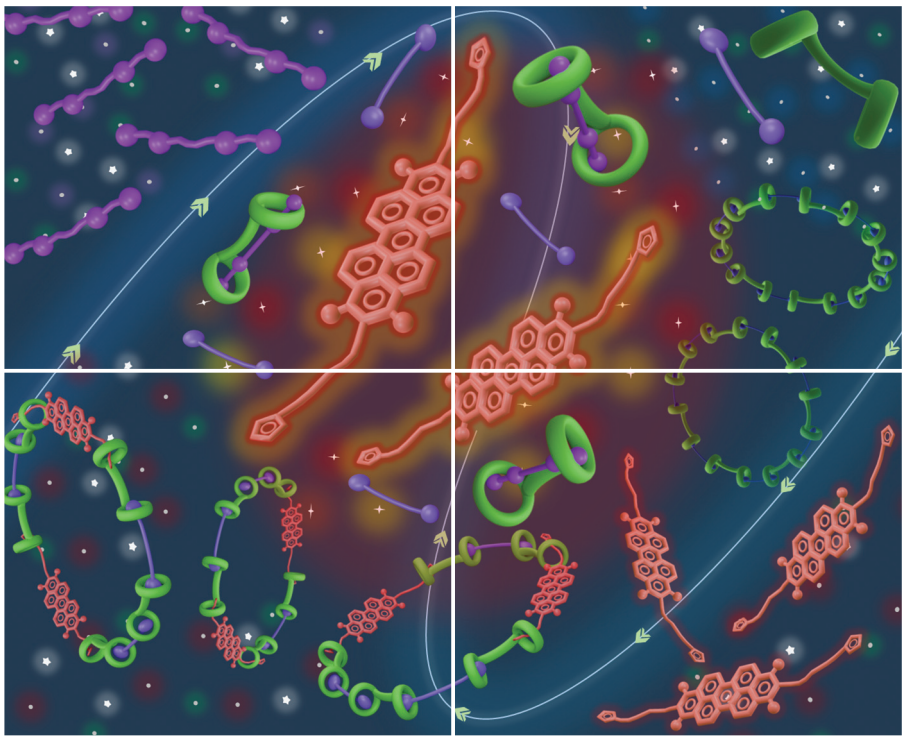

ORGANIC CHEMISTRY

FRONTIERS

CCS 中国化学会 CHINESE CHEMICAL SOCIETY

SIOC 1950

ROYAL SOCIETY OF CHEMISTRY

rsc.li/frontiers-organic

ORGANIC CHEMISTRY FRONTIERS

RESEARCH ARTICLE

View Article Online
View Journal | View Issue

Cite this: *Org. Chem. Front.*, 2024, **11**, 6293

A pillar[5]arene-based three-component supramolecular copolymer for the fluorescence detection of spermine†

Martina Mazzaferro, [a,b] Daniele Crisafulli, [a] Francesca Mancuso, [a] Marco Milone, [a] Fausto Puntoriero, [a] Anna Irto, [a] Salvatore Patanè,[c] Valentina Greco,[d] Alessandro Giuffrida,[d] Ilenia Pisagatti, *[a] Anna Notti, [a] Melchiorre F. Parisi [a] and Giuseppe Gattuso *[a]

The supramolecular polymerization of a bis-pillar[5]arene dicarboxylic acid monomer (**H**) in the presence of a mixture of complementary bis-guests 1,12-dodecanediyl-bis-1,1′-1*H*-imidazole (**G1**) and bis-*N*,*N*′-(6-(1*H*-imidazole)decyl)-perylene bisimide (**G2**), produces an AA/BB-type supramolecular copolymer **H**/**G1**/**G2** that retains the properties of the parent bi-component systems, that is, **H**/**G1** solubility and **H**/**G2** photoresponsiveness. The supramolecular copolymer showed stimuli-responsiveness, reacting to the presence of the cancer marker, spermine (**S**), by disassemblying and releasing **G2**. Once released, the perylene bisimide monomer (quenched in the copolymer by host-to-guest electron transfer), showed a remarkable increase of emission intensity. ESI-MS data are fully consistent with the formation of the **H**/**G1**/**G2** copolymer, and AFM investigations on films cast from **H**/**G1**/**G2** and **H**/**G1**/**G2** + **S** solutions demonstrated that the supramolecular copolymer sensing abilities are retained also in the solid state.

Received 9th August 2024,
Accepted 6th September 2024

DOI: 10.1039/d4qo01470g

rsc.li/frontiers-organic

Introduction

Supramolecular polymers[1–3] are ordered superstructures (or, as defined by J.-M. Lehn, 'novel expressions of complex matter'[4]) composed of monomeric units held together by non-covalent interactions rather than covalent bonds, as it happens in classical polymeric materials. They are generally prepared by the supramolecular polymerization[5–7] of small molecules that spontaneously self-assemble to produce large aggregates, that ultimately display polymeric properties.

The main advantage of these novel materials over covalent polymers is that they can be produced from a wide variety of molecular monomers, which can be chosen depending on the properties the final product must possess. In this light, both the monomer and the type of interaction that will hold the supermolecules together can in principle be customized, providing at the same time function, as brought by the molecular features of the monomer(s) of choice, as well as robustness and conditional stability, deriving from the dynamic and reversible nature of the intermolecular – *i.e.*, intermonomer – forces involved. In addition, the combination of the molecular and supramolecular properties of these materials often provides stimuli-responsiveness, the most desirable of their unique features.

Supramolecular polymers are long past the stage of scientific curiosity and have become a technological reality, with applications that span from materials science[8,9] to the biomedical field.[10–12] Research currently focus on the ability of these materials to perform specific functions in a targeted fashion. In particular, considerable effort has been devoted to the use of supramolecular polymers in the area of sensing and biosensing. Again, owing to their adaptive nature, they represent a significant advancement over conventional sensing systems based either on covalent (single-use) polymers or single-molecule reporters. In fact, supramolecular polymer sensors, in addition to the required sensitivity, selectivity and ease of read out, provide a reversibility that makes them reusable and capable of real-time monitoring of physical parameters or chemical agents. Among many, an elegant example is the

[a]*Dipartimento di Scienze Chimiche, Biologiche, Farmaceutiche ed Ambientali, Università degli Studi di Messina, Viale F. Stagno d'Alcontres, 31, 98166 Messina, Italy. E-mail: ipisagatti@unime.it, ggattuso@unime.it*
[b]*Dipartimento di Chimica, Biologia e Biotecnologie, Università degli Studi di Perugia, via Elce di Sotto, 8, 06123 Perugia, Italy*
[c]*Dipartimento di Scienze Matematiche e Informatiche, Scienze Fisiche e Scienze della Terra, Università degli Studi di Messina, Viale F. Stagno d'Alcontres 31, 98166 Messina, Italy*
[d]*Dipartimento di Scienze Chimiche, Università di Catania, Viale A. Doria 6, 95125 Catania, Italy*

†Electronic supplementary information (ESI) available: General procedures, synthetic procedure, additional NMR, PM6, TASs, ESI-MS figures, distribution diagrams, additional tables. See DOI: https://doi.org/10.1039/d4qo01470g

one reported by Schenning and co-workers,[13] an inkjet-printable sensing system based on a hydrogen-bonded supramolecular cholesteric liquid crystal network, able to return a fast response to changes in temperature and humidity by changing its reflection colour. Colour changes were determined by a change in the helix pitch as a result of water adsorption.

Supramolecular polymers can be used also for the detection of small organic molecules, as it was shown in the case of thin films formed from π-electron rich anthracene- or pyrene-containing tetracarboxylic acids.[14] Exposure to vapours of electron-deficient nitroaromatic compounds resulted in a macroscopic quenching of fluorescence, thus allowing for the detection of explosives at the level of parts per trillion (ppt).[15]

Supramolecular polymers have been also used to detect intrinsic molecular properties such as chirality. Haino and coworkers[16] reported that a porphyrin-based, hydrogen-bonded supramolecular polymer could reveal the enantiomeric excess of (+)- and (–)-α-pinene mixtures. The polymer was composed of achiral monomers that assembled in racemic (+)- and (–)-helical aggregates which reacted to the addition of nonracemic molecule with an intense response in their electronic circular dichroism spectra.

These highly representative examples show that, with the choice of suitable monomers, it is possible to program the properties of a material that has to execute a given function. When this is not directly achievable, though, it is possible to resort to blending or formulation of composite material that conjugate different properties arising from different components. It may be done by mixing supramolecular and classical covalent components (as it has been recently shown, for instance, in mechanochromic materials that display self-diagnostic properties[17,18]), or by the careful balancing of different monomers to obtain supramolecular copolymers.[19–21] These are multicomponent, non-covalently bound systems – with varying degree of internal organization[22] – comprising supramolecular domains with different molecular properties, that may even act in a synergistic manner.

Nanoarchitectures with 1D (linear) topology can be prepared by the supramolecular polymerization of heteroditopic AB-type, or pairs of complementary homoditopic AA/BB-type monomers. Among the wide range of monomeric units that have been employed,[23] those relying on host (A) and guest (B) mutual recognition are the most fascinating,[24] as a careful selection of the two counterparts may bring to the final material specific properties such as robustness, luminescence, pH responsiveness, molecular recognition *etc*.[25,26] Owing to their ease of chemical modification, crown ethers,[27,28] cyclodextrins,[29] calix[*n*]arenes,[30,31] pillar[*n*]arenes[32–34] and other macrocyclic receptors have been employed in the construction of supramolecular polymers.

In the course of our studies in this field, we have actively investigated stimuli-responsive supramolecular polymers that self-assemble as a result of host–guest interactions between calix[5]arene-[35–38] or pillar[5]arene-containing[39] monomers and complementary diaminoalkanes or alkyl(di)ammonium ions. Herein, taking advantage of the affinity between pillar[5]arenes and alkylimidazole moieties,[40,41] we describe a supramolecular copolymer composed of a novel bis-pillar[5]arene dicarboxylic acid **H** and, as complementary partners, 1,12-dodecanediyl-bis-1,1′-1*H*-imidazole **G1** and bis-*N*,*N*′-(6-(1*H*-imidazole) decyl)-perylene bisimide **G2** (Scheme 1). We will show how the **H**/**G1**/**G2** copolymer, in retaining polymers **H**/**G1** adaptivity and solubility and **H**/**G2** photophysical properties, can act as an efficient OFF/ON luminescent sensing agent for the cancer marker, spermine (**S**),[42] both in solution and in solid films.

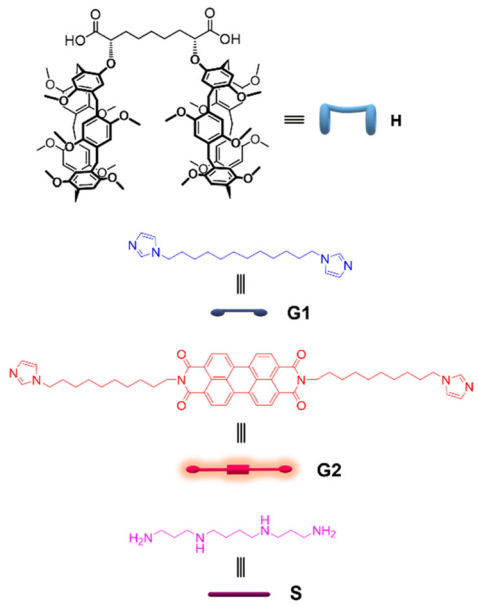

Scheme 1 Chemical structures and cartoon representation of compounds **H**, **G1**, **G2** and **S**.

Results and discussion

Synthesis of the molecular components H, G1 and G2

Bis-pillararene **H** was synthesized in two steps starting from nonamethyl-pillar[5]arene[43] **1** by following a procedure recently optimized by us for the syntheses of similar calix[5]arene[36] and pillar[5]arene[39] monomers (Scheme S1, see the ESI†). Pillararene **1** was reacted with dimethyl *meso*-2,8-dibromononandioate[44] **2** and K_2CO_3 in refluxing acetonitrile to give bis-pillararene diester **3** in 46% yield. Diester **3** was then hydrolysed to **H** using LiOH in THF/H_2O (30%). While **G1** is a known compound,[45] **G2** (Scheme S2, ESI†) was prepared from 10-(1*H*-imidazole)-1-*N*-phthalimidodecane **4**,[46] which was first converted into 10-(1*H*-imidazole)-1-decanamine **5** by treatment with hydrazine (66%), and then reacted with perylene-3,4,9,10-tetracarboxylic dianhydride **6** in refluxing DMF (80%).

H/G1 Supramolecular polymer

The ability of homoditopic **H** to act as a monomer for the self-assembly of supramolecular polymers was tested in the presence of **G1** as the complementary homoditopic partner.

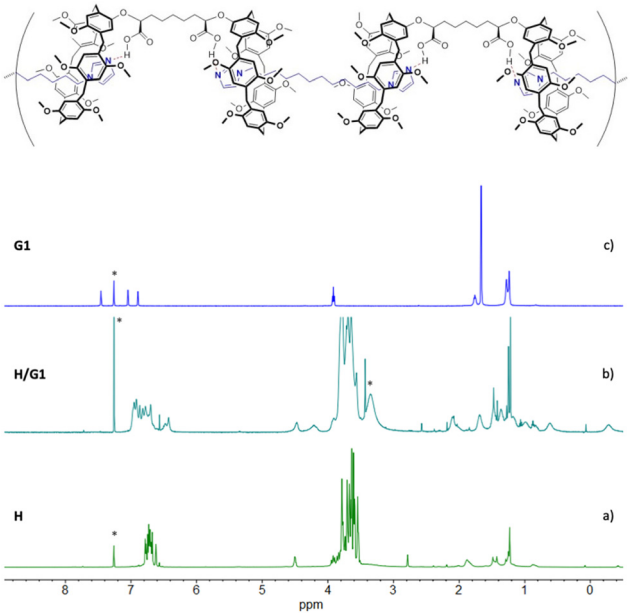

Fig. 1 ^{1}H NMR spectra (500 MHz, $CDCl_3$, 25 °C) of: (a) [**H**] = 10 mM; (b) [**H**] = [**G1**] = 10 mM; (c) [**G1**] = 10 mM. *Asterisks indicate residual solvent peaks.

Upon addition of 1 equiv. of monomer **G1** to **H**, the ^{1}H NMR resonances of the two species (Fig. 1, spectra a and c) undergo dramatic changes, confirming that the pillararene/alkylimidazole recognition is taking place. Notably, the aromatic resonances of the imidazole moieties and the aryl units present in the individual spectra of **G1** and **H** disappear, leaving room to a broad resonance (spectrum b); at the same time, two new resonances appear at high fields (δ = −0.28 and 0.62 ppm, respectively). A 2D TOCSY spectrum (Fig. S2, ESI†) allowed for the assignment of the resonances of the alkyl chains of both **G1** and **H**, showing that the high-field peaks belong to the imidazole guest placed within the cavity of a pillararene moiety experiencing – along with the adjacent methylene groups – the shielding effect of the aromatic rings of the host.

Diffusion ordered spectroscopy (DOSY) NMR experiments shed light on the self-assembly of the **H**/**G1** supramolecular polymer (Fig. S7–S10, ESI†). In keeping with previous studies,[35–39] the self-diffusion coefficients (D) of the species present in 1 : 1 samples of **H** and **G1** were found to be concentration dependent. The D values were seen to decrease consistently upon increasing the concentration of **H** and **G1** from 1.0 to 16.6 mM (D = 3.04 ± 0.08 to 1.45 ± 0.08 × 10^{-10} m^2 s^{-1}), respectively. Remarkably, over the entire concentration range investigated, both **H** and **G1** diffuse with the same coefficient, indicating the formation of **H**/**G1** aggregates (Table 1).

The average molecular mass of the aggregates can be estimated from eqn (1)[47] that, assuming the formation of random-coil, spherical-shaped supramolecular polymers,

Table 1 Self-diffusion coefficients (D) and average molecular mass (M) of **H**, diester **3** and **H**/**G1** aggregates measured at 25 °C in $CDCl_3$ in the 1.0–16.6 mM concentration range

[**H**] mM	[**G1**] mM	[**3**] mM	D (× 10^{-10} m^2 s^{-1})	M (amu)
1	1	—	3.04 ± 0.08	5350
5	5	—	2.43 ± 0.09	8250
10	10	—	1.84 ± 0.09	24 100
16.6	16.6	—	1.45 ± 0.08	49 300
16.6	—	—	3.87 ± 0.08	2600
—	—	16.6	4.50 ± 0.09	1684

inversely correlates the self-diffusion coefficient D with the molecular mass M:

$$D_{\text{aggregate}}/D_{\text{monomer}} = (M_{\text{monomer}}/M_{\text{aggregate}})^{1/3} \quad (1)$$

Given the natural tendency of carboxylic acids to form hydrogen-bonded dimers (especially in aprotic solvents such as $CDCl_3$), the self-diffusion coefficients of **H** and the diester precursor **3** were measured and compared (Fig. S11, ESI†). The latter was found to diffuse with a D = 4.50 ± 0.09 × 10^{-10} m^2 s^{-1}, indicating that **H** (D = 3.87 ± 0.08 × 10^{-10} m^2 s^{-1}) is in equilibrium with its dimeric form. Simple calculations (using the D value of **3** as the reference value for a monomeric bis-pillar[5]arene) show that at 1 mM the **H**/**G1** aggregates have an average M = 5350 amu whereas at 16.6 mM the average M increases to 49 300 amu, roughly corresponding to an increase from *ca.* 3 to 25 **H**/**G1** monomeric units.

H/G2 Supramolecular system

Perylene bisimide-containing monomer **G2** was found to be sparingly soluble in $CHCl_3$, preventing further studies on the **H**/**G2** polymer in the millimolar range to allow for NMR characterization. However, the interaction between **H** and **G2** could conveniently be investigated by UV-vis and fluorescence spectroscopy (Fig. 2). To this end, a **G2** solution (7.83 × 10^{-6} M in $CHCl_3$/CF_3CH_2OH (TFE) 97 : 3 v/v, *vide infra*) was titrated with a solution of bis-pillar[5]arene **H**. Progressive additions of **H** caused a corresponding hyperchromic effect on the band at

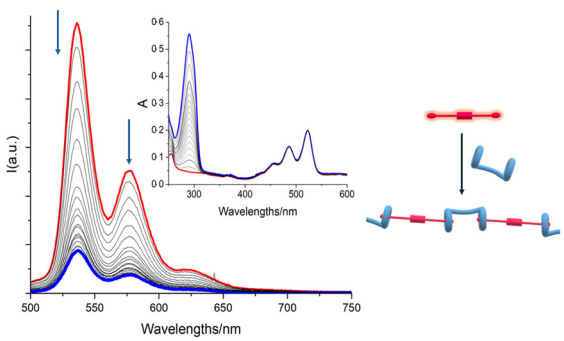

Fig. 2 Emission and absorption (inset) titrations in $CHCl_3$/TFE 97 : 3 v/v of [**G2**] = 7.83 × 10^{-6} M with [**H**] = 2.46 × 10^{-4} M solution (titrant concentration from 7.78 × 10^{-7} to 1.54 × 10^{-5} M). The excitation wavelength was set at λ_{ex} = 456 nm.

λ = 292 nm belonging to the pillar[5]arene macrocycle, without affecting the absorption spectrum of **G2** (characterized by the typical perylene bisimide absorptions in the 420–540 nm spectral range), thus indicating that the ground-state of the perylene bisimide moiety is not affected.

The emission spectrum of **G2** (λ_{ex} = 456 nm) features the three typical bands of perylene bisimide moieties at λ = 537, 578 and 627 nm, respectively. Upon addition of **H**, the fluorescence intensity of **G2** was progressively quenched as the titration proceeded, probably as result of a host-to-guest photoinduced electron transfer (PET), favoured by the tendency of the perylene bisimide moiety to behave as a good electron acceptor (owing to its relatively low reducing potential).[48–50]

To evaluate in detail the effect of complexation on the photophysical properties of perylene bisimide, pump–probe transient absorption experiments were carried out by exciting at 400 nm (100 fs) a solution of **H**/**G2**. The transient absorption spectra (TAS) are shown in Fig. 3.

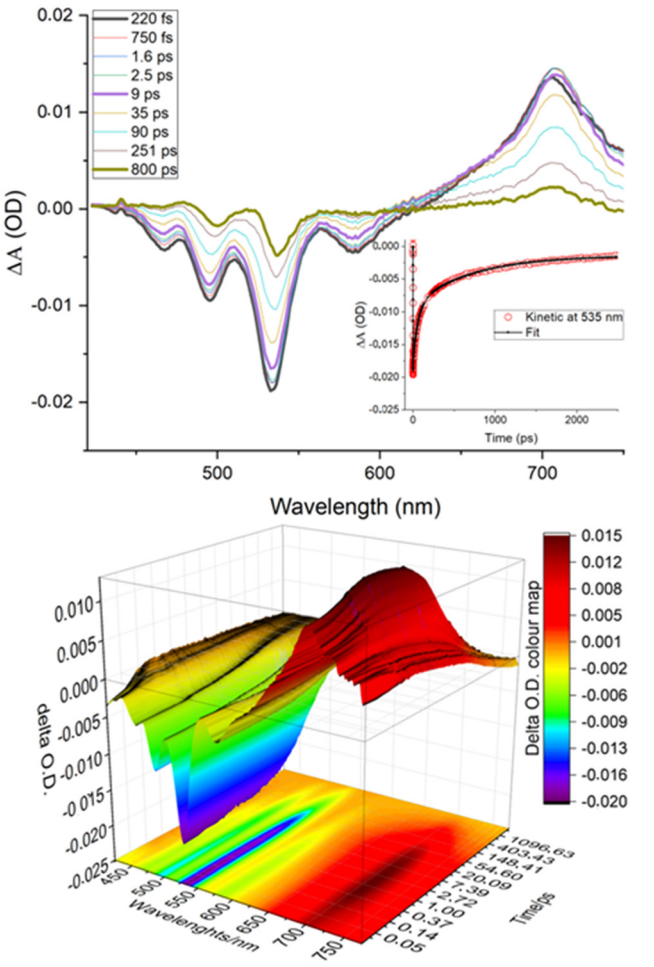

Fig. 3 TAS matrix (bottom) and selected TASs (top) with kinetic fitting @ 530 nm in the inset (top) of [**H**/**G2**] = 3.83 × 10^{-5} M in $C_2H_2Cl_4$/TFE 97 : 3 v/v solution. Chloroform was replaced with tetrachloroethane to avoid the formation of HCl under high-energy laser light excitation. The excitation wavelength was set at λ_{ex} = 400 nm (pulse 100 fs, 100 mJ).

The initial spectrum showed the characteristic bands of a perylene bisimide. Bleaching could be observed in the region between 420 and 540 nm and a stimulated emission contribution at lower energy, while above 600 nm an intense absorption typical of perylene bisimides could be distinguished.[49,51]

The spectrum of the optically populated species evolved in about 9 ps, albeit with little spectral variation, to a new species characterized by a weak absorption around 620 nm. The evolution of TAS remained almost constant in the first 90 ps, to leave the field to a spectrum, weak in intensity, attributable to a small fraction of the sample, that evolved with a lifetime on the order of 900 ps.

To rationalize these results, it should be kept in mind that pillararenes may undergo an oxidation process at about 0.75 V *vs.* Fc (*ferrocenium*/*ferrocene*) while perylene bisimides undergo a reduction process at potentials less negative than −1 V *vs.* Fc.[49,51]

The excited state energy for **G2**, evaluated from the intersection of the normalized absorption and emission spectra, resides at approximately 2.4 eV. Using the simplified Rehm–Weller equation[52] it is possible to estimate the driving force for the photoinduced electron transfer process from the pillararene to the fluorophore which, despite all the used approximations, turns out to be strongly negative of about 0.7 eV.

In order to gain additional evidence, TAS experiments were carried out by recording the spectral changes in the near infrared and, as shown in Fig. S17, ESI,† within a few ps the formation of a peak at about 950 nm assignable (by comparison with literature data[51]) to the formation of the reduced **G2** by the pillararene is observed and this species recombines to the fundamental state within about 100 ps, while an absorption tail is recovered on a longer time scale (about 1 ns).

Taken together, these results suggest that the excited state of **G2** in the complexed form is quenched by electron transfer from the pillararene with a time constant of 8.6 ps and the charge-separated state so formed recombines with a time constant of about 85 ps.

The signal that evolves in a longer time scale can be attributed to the non-complexed portion of **G2** or to a remote electron transfer effect from a pillararene cavity that is not directly complexed, but still in close proximity to the fluorophore. This species evolves with a time constant comparable to that of the residual luminescent excited state, which is found to be about 1 ns.

With the aim of testing the **H**/**G2** system for a potential use as the sensing component in a biomedical device, a 3 : 1 **H**/**G2** solution in $CHCl_3$/TFE 97 : 3 v/v (excess **H** was added to make sure that **G2** was conveniently quenched) was treated with increasing amounts of spermine (**S**). While the UV-vis absorption spectra showed no change whatsoever (Fig. 4), emission spectra showed a progressive increase of emission intensity (Fig. 4), indicating that **G2** was being released from the pillararene cavities and it was regaining its emission properties, confirming that **S** may efficiently act as competitor for the bispillar[5]arene **H**, and therefore the **H**/**G2** system may successfully act as a sensing agent for spermine detection.

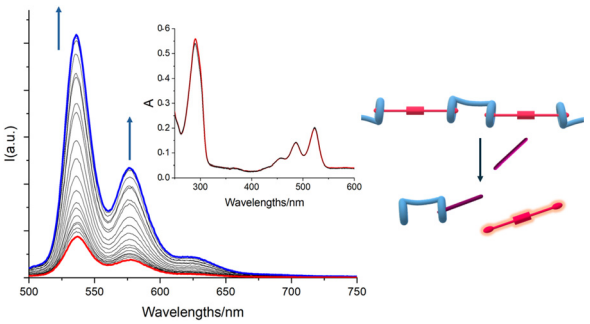

Fig. 4 Absorption and emission (inset) titrations in $CHCl_3$/TFE 97 : 3 v/v of a solution containing [**G2**] = 7.34 × 10^{-4} M and [**H**] = 2.19 × 10^{-3} M with a [**S**] = 2.3 × 10^{-4} M solution (titrant concentration from 7.73 × 10^{-7} to 1.57 × 10^{-5} M). The excitation wavelength was set at λ_{ex} = 456 nm.

H/G1/G2 Supramolecular copolymer

The construction of a functioning device requires the incorporation of the sparingly soluble **H**/**G2** sensing system into an adaptive and easy-to-handle backbone. It was therefore envisaged that formulation of a three component **H**/**G1**/**G2** copolymer could provide a material retaining both the **H**/**G1** stability and **H**/**G2** sensing properties. The copolymer was prepared by solid–liquid extraction of **G2** with a solution of preformed **H**/**G1** oligomers, containing a slight excess of **H** over **G1** (1 : 0.9 host-to-guest ratio). Therefore, a [**H**] = 10 mM, [**G1**] = 9 mM in a $CDCl_3$/TFE (97 : 3 v/v) solution was stirred for 2 h at room temperature in the presence of an excess of solid **G2**, and then filtered through a 0.45 μm PTFE membrane.

^{1}H NMR spectra in Fig. 5 show that, after the extraction (spectrum c), the resonances of free **G2** (spectrum d) underwent significant changes. The multiplet belonging to the perylene aromatic core (δ = 8.58–8.71 ppm) broadened, whereas the imidazole ring hydrogen atoms shifted up-field, merging with the broad resonance assigned to the pillararene aromatic hydrogen atoms. In addition, comparison between spectra (b) and (c) shows the appearance of a second set of resonances in the high field region consistent with the methylene groups of **G2** included inside the aromatic cavities of the pillararene macrocycles (as demonstrated by a 2D TOCSY spectrum where the methylene chains of the three monomers are clearly identified, see Fig. S3 and S4, ESI†). Integration of the relevant peaks at δ = 4.43 ppm (for **H**), δ = –0.11 ppm (for **G1**) and δ = –0.28 ppm (for **G2**) in spectrum 5c confirms the 1 : 0.9 : 0.1 composition of the copolymer.

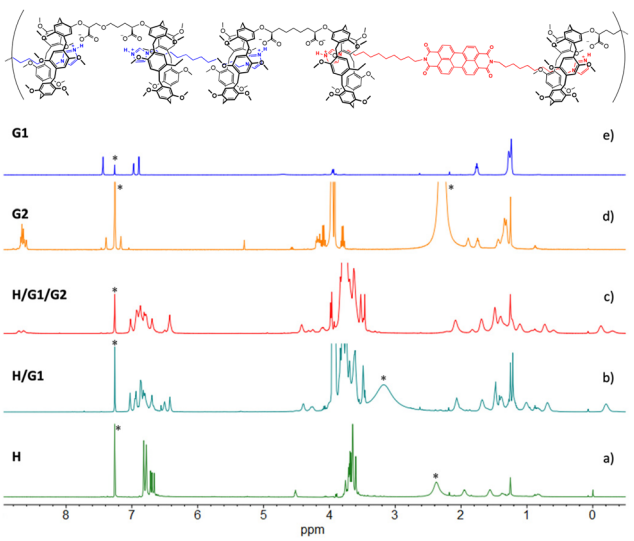

Fig. 5 ^{1}H NMR spectra (500 MHz, 25 °C, $CDCl_3$/TFE, 97 : 3, v/v) of: (a) [**H**] = 10 mM; (b) [**H**] = [**G1**] = 10 mM; (c) [**H**] = 10 mM, [**G1**] = 9 mM, [**G2**] = 1 mM; (d) [**G2**] = 0.6 mM. *Asterisks refer to residual solvent peaks.

A series of DOSY NMR spectra provided conclusive evidence on the **H**/**G1**/**G2** copolymer formation, rather than the coexistence of a mixture of **H**/**G1** and **H**/**G2** aggregates (Fig. 6). Careful inspection of Fig. 6c reveals that all the components of the copolymer diffuse with the same coefficient, indicating that they belong to the same aggregate and that they are not diffusing independently. Moreover, the diffusion coefficient of the **H**/**G1**/**G2** copolymer (D = 1.47 ± 0.06 × 10^{-10} m^2 s^{-1}, at [**H**] = 10 mM, [**G1**] = 9 mM and [**G2**] = 1 mM in $CDCl_3$/TFE, 97 : 3, v/v, Table 2, see also Fig. S12–14, ESI†) was found to be smaller than the one measured at the same concentration for the **H**/**G1** polymer (1.83 ± 0.05 × 10^{-10} m^2 s^{-1}), showing that the addition of TFE (that improves **G2** solubility) led to an increase of the average molecular mass from M = 24 500 to 47 300 amu. In fact, in line with previous studies,[39,53] protic solvents promote host-to-guest proton transfer, with the result that electrostatic attraction between the charged moieties ($COO^-\cdots HN^+$) increase the affinity of the pillararene cavity for the guest monomers.‡ Diacid **H** in this solvent mixture was found to diffuse with a D very close to that of the diester **3**, which in turn was found to diffuse with same coefficient as in neat $CDCl_3$.

The effect of spermine on the supramolecular copolymer **H**/**G1**/**G2** was initially investigated by ^{1}H NMR (Fig. 7). Addition of up to 2 eq. of **S** led to dramatic changes (spectrum b): the resonances for both included **G1** and **G2** methylene groups disappeared, and the peaks for the free imidazole ring(s) reappeared in the aromatic region of the spectrum. Likewise, no free spermine resonances were seen in spectrum b, indicating that it was recognized and complexed by the pillar[5]arene cavities of **H**.§

‡ Previous studies[39] on the self-assembly of supramolecular polymers from analogous bis-pillar[5]arene dicarboxylic acids and α,ω-diaminoalkanes showed that, upon recognition, proton transfer from the host to the guest[64] takes place if a protic solvent (*e.g.*, trifluoroethanol (TFE), 3–10% v/v) is added to the chloroform solution containing both monomers, whereas no proton transfer can be observed in neat chloroform. In the present case, addition of trifluoroethanol to a **H**/**G1** solution in $CDCl_3$ result in the COOH group of the host protonating the basic imidazole nitrogen atom of the guest, as confirmed by the tell-tale upfield shift (from δ = 4.47 to 4.40 ppm) of the resonance belonging to the CH group adjacent to the carboxyl moiety (Fig S1, ESI,† shows the optimized geometry of the repeating unit of the **H**/**G1** aggregate). This topic has been extensively reviewed recently.[53]

§ Linear (poly)amines are efficiently recognized by carboxyl-bearing receptors. Host-to-guest proton transfer has been demonstrated as a powerful tool for the formation of internally ion-paired complexes.[53,65–67]

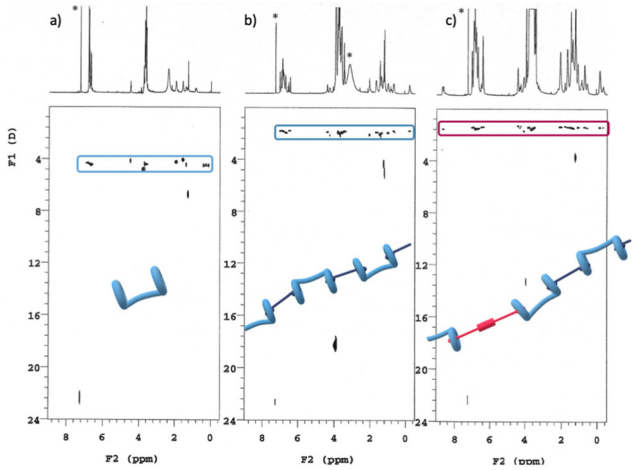

Fig. 6 DOSY plots (500 MHz, 25 °C, $CDCl_3$/TFE, 97 : 3, v/v) of (a): [**H**] = 10 mM; (b) [**H**] = [**G1**] = 10 mM; (c) [**H**] = 10 Mm, [**G1**] = 9 mM, [**G2**] = 1 mM. *Asterisks refer to residual solvent peaks.

Table 2 Diffusion coefficients (*D*) and average molecular mass (M) of **H**, diester **3**, **H**/**G1** and **H**/**G1**/**G2** aggregates measured at 25 °C in $CDCl_3$/TFE, 97 : 3, v/v

[**H**] mM	[**G1**] mM	[**G2**] mM	[**3**] mM	*D* ($\times 10^{-10}$ m^2 s^{-1})	*M* (amu)
10	10	—	—	1.83 ± 0.05	24 500
5	4.5	0.5	—	1.91 ± 0.09	21 600
10	9	1	—	1.47 ± 0.06	47 300
10	—	—	—	4.41 ± 0.05	1780
—	—	—	10	4.50 ± 0.09	1684

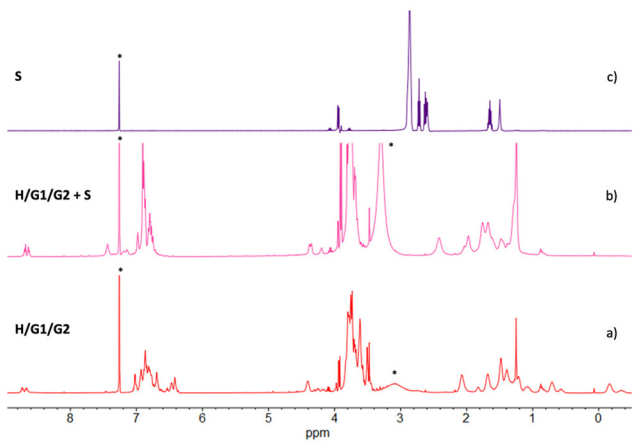

Fig. 7 ^{1}H NMR spectra (500 MHz, 25 °C, $CDCl_3$/TFE, 97 : 3, v/v) of (a) [**H**] = 5 mM, [**G1**] = 4.5 mM, [**G2**] = 0.5 mM; (b) [**H**] = 5 mM, [**G1**] = 4.5 mM, [**G2**] = 0.5 mM, [**S**] = 10 mM; (c) [**S**] = 10 mM. *Asterisks refer to residual solvent peaks.

DOSY experiments confirmed the conclusions drawn from ^{1}H NMR data (Fig. 8): addition of spermine results in the disassembly of the supramolecular copolymer. In fact, all the single species present in solution diffuse with a different self-diffusion coefficient, as expected for a mixture of compounds

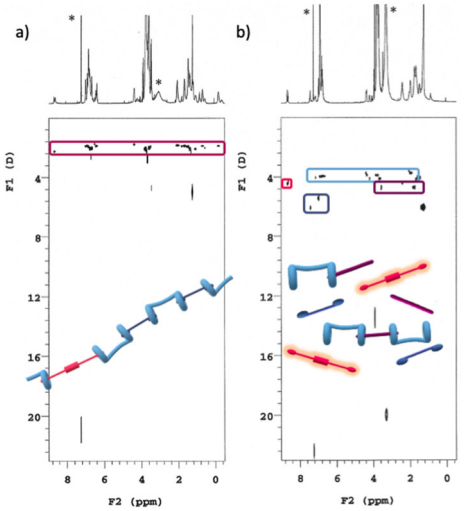

Fig. 8 DOSY plots (500 MHz, 25 °C, $CDCl_3$/TFE, 97 : 3, v/v) of (a) [**H**] = 5 mM, [**G1**] = 4.5 mM, [**G2**] = 0.5 mM; (b) [**H**] = 5 mM, [**G1**] = 4.5 mM, [**G2**] = 0.5 mM, [**S**] = 10 mM. *Asterisks refer to residual solvent peaks.

not interacting with each other and definitively not belonging to the same supramolecular species. In addition, the appearance in the TOCSY spectrum of the same mixture of spectra 7b and 8b (Fig. S5, ESI†) of seven cross-peaks (belonging to the central alkyl chain of a non-symmetrically complexed bis-pillararene) demonstrated that a 1 : 1 **H**/**S** is formed upon copolymer disaggregation.

The conclusive evidence on the ability of the **H**/**G1**/**G2** copolymer to respond to and to reveal spermine **S** was provided by UV-vis and fluorescence data (Fig. 9). Again, while absorption

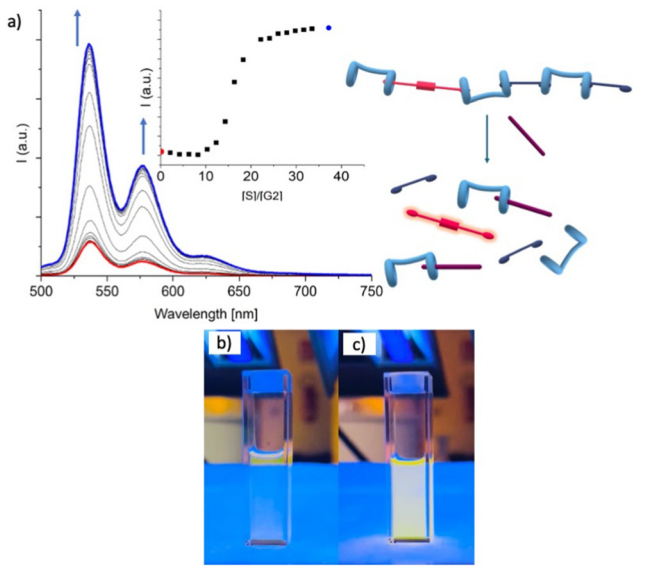

Fig. 9 (a) Emission titration in $CHCl_3$/TFE 97 : 3 v/v of a solution containing [**G1**] = 1.01 × 10^{-5} M, [**G2**] = 1.13 × 10^{-6} M and [**H**] = 1.13 × 10^{-5} M with a [**S**] = 1.54 × 10^{-3} M solution (titrant concentration from 6.0 × 10^{-6} to 1.0 × 10^{-4} M). The excitation wavelength was set at λ_{ex} = 456 nm. Inset: emission intensity as a function of [**S**]/[**G2**] ratio. Pictures (b) and (c) show the cuvette at the beginning and at the end of the titration.

spectra do not change significantly upon addition of **S**, emission spectra sharply increase in intensity when a 9 : 1 **S**/**G2** molar ratio (*e.g.* 1 : 1 **S**/**G1**) is reached, suggesting that the displacement of **G2** begins only after **G1** is fully released. This observation also showed that upon release from the copolymer backbone, **G2** fluorescence is switched on, confirming that the optical properties of the **H**/**G2** sensing system are fully retained even when incorporated in the copolymer.

Such a progressive displacement was explained by a series of ^{1}H NMR titrations that, combined with the emission titrations, allowed us to quantify the strength, in terms of formation constants, of the different diads (AB) and triads (ABA, BAB) contained in the copolymer backbone (*i.e.*, **H**/**G1**, **H**/**G2**, **G1**/**H**/**G1**, **G2**/**H**/**G2**, **H**/**G1**/**H** and **H**/**G2**/**H**). Data treatment provided the formation constants reported in Table 3 (for full details see Tables S1 and S2, ESI†).

K for the **H**/**G1** and **H**/**G2** complexes are very close, indicating that the 1 : 1 interaction between the pillararene cavity and the alkylimidazole guest moiety – after host-to-guest proton transfer – is not significantly influenced by the remaining parts of the **G1** and **G2** guest monomers.¶ Little difference is also seen for the **H**-centered **G1**/**H**/**G1** and **G2**/**H**/**G2** triads ($1.17 \pm 0.08 \times 10^5$ and $2.51 \pm 0.17 \times 10^4$, respectively), showing that the complexation of two alkylimidazole by a single ditopic **H** monomer is marginally influenced by the recognition events taking place in the two pillararene cavities. On the other hand, a remarkable difference is seen for the ABA (guest-centered) triads. **H**/**G1**/**H** is formed from **H**/**G1** with a $K = 3.02 \pm 0.56 \times 10^2$ M^{-1}, whereas **H**/**G2**/**H** is formed from **H**/**G2** with a $K = 1.74 \pm 0.12 \times 10^6$ M^{-1}, revealing that the 'weak' link where the attack of the spermine analyte takes place is the **H**/**G1**/**H** unit, probably because **G1** is too short to avoid steric repulsion between the pillararene moieties of two different **H** units encircling the two ends of a **G1** monomer (**H**/**G1**/**H** has a much lower percentage of formation than **H**/**G2**/**H**, see also the distribution diagrams in Fig. S19 and S20, ESI†). This evidence also explains the reason why **G2** is released only after all **G1** molecules have been replaced by **S**. Furthermore, even though **S** binds to **H** with a $K = 2.45 \pm 0.06 \times 10^6$, comparable to the one of the **H**/**G1** and **H**/**G2** complexes, smoothly displaces both **G1** and **G2**, being primary amines by far more basic than imidazole.[54–57] Remarkably, the chemical shifts observed during the titrations and the calculated ones are in excellent agreement, (Fig. S18, ESI†).

Mass spectrometry experiments allowed to further elucidate the interactions between spermine and the supramolecular copolymer. Analysis of the ESI-MS spectra corroborated data previously acquired by DOSY NMR (Fig. 10). In particular, the observation of peaks at *m*/*z* 1961.1 and 984.9, corresponding to the $[\mathbf{H} + \mathbf{G1} + H]^+$ ion and the $[2\mathbf{H} + 2\mathbf{G1} + H_2O + 4H]^{4+}$ multicharged ion, as well as *m*/*z* 2461.3 and 1234.9, corresponding to the $[\mathbf{H} + \mathbf{G2} + H]^+$ and $[2\mathbf{H} + 2\mathbf{G2} + H_2O + 4H]^{4+}$ ions, respectively, confirmed the formation of 1 : 1 and 2 : 2 complexes within the two distinct polymer systems (see Fig. S21–S24 for details†). The same species were observed in the spectrum of the **H**/**G1**/**G2** copolymer.‖

Furthermore, the interaction between **H** and spermine (**S**) was investigated by ESI-MS,[58,59] and the formation of 1 : 1 **H**/**S** and larger complexes was confirmed by the observation of peaks at *m*/*z* 1862.4 and 935.4, corresponding to the $[\mathbf{H} + \mathbf{S} + H]^{2+}$ and $[2\mathbf{H} + 2\mathbf{S} + H_2O + 4H]^{4+}$ ions, respectively.‖ The displacement of **G2** was demonstrated by treating the **H**/**G1**/**G2** supramolecular copolymer with **S**. Subsequent analysis, under identical experimental conditions, clearly showed **H**/**S** complex formation.

Atomic Force Microscopy (AFM) and Raman spectroscopy shed further light on the ability of the **H**/**G1**/**G2** copolymer to reveal spermine even in the solid state.[60,61] As a preliminary screening, Raman spectra were collected for the three components and the copolymer (Fig. 11), revealing that both **G2** and **H**/**G1**/**G2** copolymer display between 1300 and 1600 cm^{-1}

Table 3 Formation constants (*K*) for the diads and triads present in the **H**/**G1**/**G2** copolymer and for the **H**/**S** complex calculated from emission titrations in $CHCl_3$/TFE 97 : 3 v/v or ^{1}H NMR titrations in $CDCl_3$/TFE 97 : 3 v/v (see Tables S1, S2, Fig. S15, S16 and S18–S20, ESI, for full details†)

Complex	log β	log K	K (M^{-1})
H/**G1**[a]	6.03 ± 0.01	6.03 ± 0.01	$1.07 \pm 0.05 \times 10^6$
H/**G2**[b]	6.42 ± 0.01	6.42 ± 0.01	$2.69 \pm 0.06 \times 10^6$
H/**G1**/**H**[a]	8.51 ± 0.07	2.48 ± 0.08	$3.02 \pm 0.56 \times 10^{2c}$
G1/**H**/**G1**[a]	11.10 ± 0.02	5.07 ± 0.03	$1.17 \pm 0.08 \times 10^{5c}$
H/**G2**/**H**[b]	12.66 ± 0.02	6.24 ± 0.03	$1.74 \pm 0.12 \times 10^{6c}$
G2/**H**/**G2**[b]	10.80 ± 0.02	4.40 ± 0.03	$2.51 \pm 0.17 \times 10^{4c}$
H/**S**[a]	6.39 ± 0.01	6.39 ± 0.01	$2.45 \pm 0.06 \times 10^6$
S/**H**/**S**[a]	10.08 ± 0.01	3.69 ± 0.02	$4.90 \pm 0.20 \times 10^{3c}$

[a] Determined by ^{1}H NMR. [b] Determined by emission data. [c] These constants refer to **HX** + **H** → **H$_2$X** or **HX** + **X** → **HX$_2$** equilibria (**X** = **G1**, **G2** or **S**).

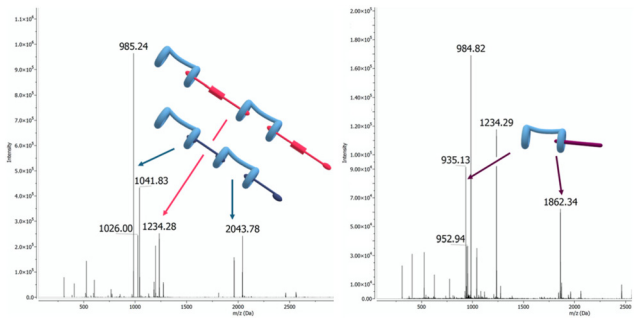

Fig. 10 ESI-MS(+) spectra of left: **H**/**G1**/**G2** ([**H**] = 10 μM, [**G1**] = 9 μM, [**G2**] = 1 μM), and right: **H**/**G1**/**G2** treated with **S** ([**S**] = 10 μM).

¶The association constant of decamethyl-pillar[5]arene and 1-decylimidazole was reported to be $2.3 \pm 0.2 \times 10^2$ M^{-1}, whereas between decamethyl-pillar[5]arene and 1-decylimidazolium trifluoroacetate was $1.0 \pm 0.3 \times 10^4$ M^{-1} in chloroform.[41] Proton-transfer mediated recognition explain the higher stability (>10^6 M^{-1}) of the **H**/**G1** and **H**/**G2** complexes.

‖Given the tendency of these polymeric systems to aggregate, the formation of larger multicharged ions (*e.g.*, $[2\mathbf{H} + 2\mathbf{G1} + 2H]^{2+}$) cannot be ruled out.

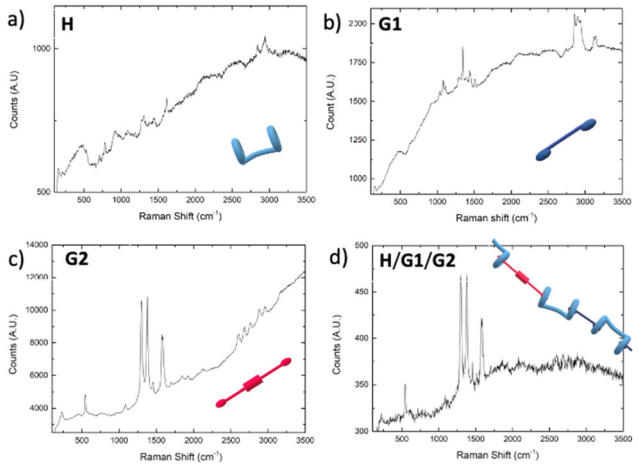

Fig. 11 Raman spectra collected from solids deposited on silica surface from solutions ($CHCl_3$/TFE, 97 : 3, v/v): (a) [**H**] = 3 mM; (b) [**G1**] = 2.7 mM; (c) [**G2**] = 0.3 mM; (d) [**H**] = 3 mM, [**G1**] = 2.7 mM, [**G2**] = 0.3 mM.

the typical Raman bands of perylene bisimide moieties (corresponding to C–H bending and C=C stretching, respectively),[62,63] thus confirming that, also in the film, **G2** is still part of the copolymer. Emission spectra recorded on **G2** (which forms small clusters upon evaporation, Fig. 12a), and **H**/**G1**/**G2** films (Fig. 12b) showed that the perylene bisimide fluorophore is quenched in the copolymer film but it provides an intense emission when cast as the free species.

Finally, deposition of a solution containing the copolymer **H**/**G1**/**G2** containing 2 eq. of spermine **S** produced a grid-like film in which **G2** fluorescence has been restored (Fig. 13), demonstrating the viability of the supramolecular copolymer for the incorporation into sensing devices.

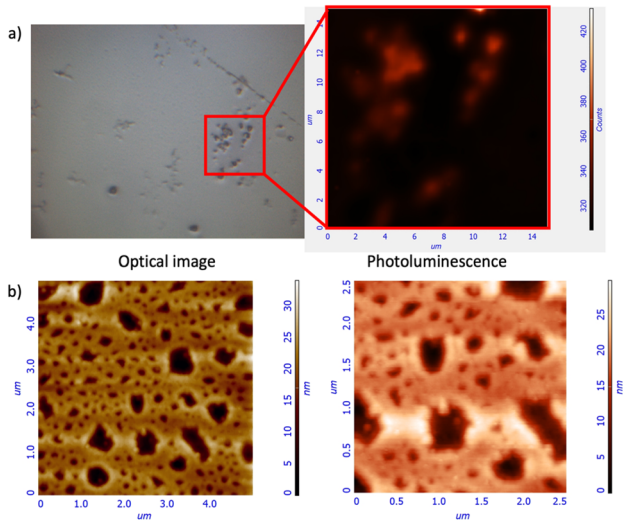

Fig. 12 (a) Photoluminescence observed upon irradiation at λ_{ex} = 472 nm of a cluster of **G2**. (b) AFM topography image of the grid obtained upon spin-coating of a [**H**] = 3 mM, [**G1**] = 2.7 mM, [**G2**] = 0.3 mM solution ($CHCl_3$/TFE, 97 : 3, v/v) onto a silica surface.

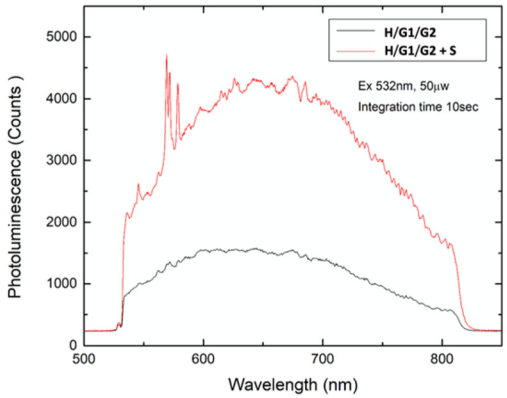

Fig. 13 Emission spectra recorded on solid films obtained from [**H**] = 3 mM, [**G1**] = 2.7 mM, [**G2**] = 0.3 mM (black line), and [**H**] = 3 mM, [**G1**] = 2.7 mM, [**G2**] = 0.3 mM, [**S**] = 6 mM (red line) solutions.

Conclusions

Data presented in this paper show that the supramolecular copolymer herein self-assembled from three monomers – a bis-pillar[5]arene dicarboxylic acid (**H**), a dodecanediyl-bis-imidazole (**G1**) and a bis-*N*,*N*′-imidazoledecyl-perylene bisimide (**G2**) retained both the solubility and adaptability of the **H**/**G1** polymer and the OFF/ON fluorescence detection ability of the **H**/**G2** system. This material was shown, by a variety of techniques, to be able to efficiently detect the cancer marker, spermine (**S**) in solution, as a result of a progressive displacement/disassembly process that restores the fluorescence of the perylene bis-imide signalling unit.

The results presented demonstrate a key concept: formulation of supramolecular copolymers opens up avenues for the facile development of complex materials that may conjugate properties from different components, avoiding tiresome syntheses in favour of an easy approach of readily-made monomers 'pick-and-mix.'

Further investigations will be aimed at the development of a portable sensing device for the direct detection of spermine in biological fluids, and to the assessment of the supramolecular copolymer potential as a carrier in drug-delivery.

Author contributions

Conceptualization: G. G., I. P.; data curation: A. I., F. P.; formal analysis: A. I., M. Mi., A. G., F. P., S. P.; funding acquisition: G. G., M. F. P., A. N.; investigation: M. Ma., D. C., F. M., M. Mi., V. G., S. P.; project administration: G. G., I. P., F. P.; resources: M. Ma., D. C.; supervision: I. P., M. F. P., A. N., F. P., A. G.; validation: I. P., F. P.; visualization: D. C., M. Ma.; writing – original draft: G. G., I. P., F. P.; writing – review & editing: G. G., M. F. P.

Data availability

The data supporting this article have been included as part of the ESI.†

Conflicts of interest

There are no conflicts to declare.

Acknowledgements

This work was partially funded by the European Union (NextGeneration EU), through the MUR-PNRR project SAMOTHRACE (SiciliAn MicronanOTecH Research And Innovation CEnter, ECS00000022).

References

1 U. S. Schubert, G. R. Newkome and A. Winter, *Supramolecular Polymers and Assemblies – From Synthesis to Properties and Application*, Wiley-VCH, Weinheim, 2021.
2 A. J. Savyasachi, O. Kotova, S. Shanmugaraju, S. J. Bradberry, G. M. O'Máille and T. Gunnlaugsson, Supramolecular Chemistry: A Toolkit for Soft Functional Materials and Organic Particles, *Chem*, 2017, **3**, 764–811.
3 L. Yang, X. Tan, Z. Wang and X. Zhang, Supramolecular Polymers: Historical Development, Preparation, Characterization, and Functions, *Chem. Rev.*, 2015, **115**, 7196–7239.
4 J.-M. Lehn, Perspectives in Chemistry—Aspects of Adaptive Chemistry and Materials, *Angew. Chem., Int. Ed.*, 2015, **54**, 3276–3289.
5 T. F. A. De Greef, M. M. J. Smulders, M. Wolffs, A. P. H. J. Schenning, R. P. Sijbesma and E. W. Meijer, Supramolecular Polymerization, *Chem. Rev.*, 2009, **109**, 5687–5754.
6 P. K. Hakshim, J. Bergueiro, E. W. Meijer and T. Aida, Supramolecular Polymerization: A Conceptual Expansion for Innovative Materials, *Prog. Polym. Sci.*, 2020, **105**, 101250.
7 J. Matern, Y. Dorca, L. Sańchez and G. Fernańdez, Revising complex supramolecular polymerization under kinetic and thermodynamic control, *Angew. Chem., Int. Ed.*, 2019, **58**, 16730–16740.
8 F. Xu and B. L. Feringa, Photoresponsive Supramolecular Polymers: From Light-Controlled Small Molecules to Smart Materials, *Adv. Mater.*, 2023, **35**, 2204413.
9 A. D. O'Donnell, S. Salimi, L. R. Hart, T. S. Babra, B. W. Greenland and W. Hayes, Applications of supramolecular polymer networks, *React. Funct. Polym.*, 2022, **172**, 105209.
10 D. Wang, G. Tong, R. Dong, Y. Zhou, J. Shen and X. Zhu, Self-assembly of supramolecularly engineered polymers and their biomedical applications, *Chem. Commun.*, 2014, **50**, 11994–12017.
11 R. Dong, Y. Zhou, X. Huang, X. Zhu, Y. Lu and J. Shen, Functional Supramolecular Polymers for Biomedical Applications, *Adv. Mater.*, 2015, **27**, 498–526.
12 X. Li, M. Shen, J. Yang, L. Liu and Y.-W. Yang, Pillararene-Based Stimuli-Responsive Supramolecular Delivery Systems for Cancer Therapy, *Adv. Mater.*, 2024, **36**, 2313317.
13 N. Herzer, H. Guneysu, D. J. D. Davies, D. Yildirim, A. R. Vaccaro, D. J. Broer, C. W. M. Bastiaansen and A. P. H. J. Schenning, Printable Optical Sensors Based on H-Bonded Supramolecular Cholesteric Liquid Crystal Networks, *J. Am. Chem. Soc.*, 2012, **134**, 7608–7611.
14 B. Gole, S. Shanmugaraju, A. K. Bar and P. S. Mukherjee, Supramolecular polymer for explosives sensing: role of H-bonding in enhancement of sensitivity in the solid state, *Chem. Commun.*, 2011, **47**, 10046–10048.
15 B. Gole, W. Song, M. Lackinger and P. S. Mukherjee, Explosives Sensing by Using Electron-Rich Supramolecular Polymers: Role of Intermolecular Hydrogen Bonding in Significant Enhancement of Sensitivity, *Chem. – Eur. J.*, 2014, **20**, 13662–13680.
16 T. Hirao, S. Kishino and T. Haino, Supramolecular chiral sensing by supramolecular helical polymers, *Chem. Commun.*, 2023, **59**, 2421–2424.
17 Y. Sagara, M. Karman, A. Seki, M. Pannipara, N. Tamaoki and C. Weder, Rotaxane-Based Mechanophores Enable Polymers with Mechanically Switchable White Photoluminescence, *ACS Cent. Sci.*, 2019, **5**, 874–881.
18 A. E. Früh, F. Artoni, R. Brighenti and E. Dalcanale, Strain Field Self-Diagnostic Poly(dimethylsiloxane) Elastomers, *Chem. Mater.*, 2017, **29**, 7450–7457.
19 L. Albertazzi, N. van der Veeken, M. B. Baker, A. R. A. Palmans and E. W. Meijer, Supramolecular copolymers with stimuli- responsive sequence control, *Chem. Commun.*, 2015, **51**, 16166–16168.
20 H. Frisch, E.-C. Fritz, F. Stricker, L. Schmüser, D. Spitzer, T. Weidner, B. J. Ravoo and P. Besenius, Kinetically Controlled Sequential Growth of Surface-Grafted Chiral Supramolecular Copolymers, *Angew. Chem., Int. Ed.*, 2016, **55**, 7242–7246.
21 H. Li, Y. Yang, F. Xu, Z. Duan, R. Li, H. Wen and W. Tian, Sequence-controlled supramolecular copolymer constructed by self-sorting assembly of multiple noncovalent interactions, *Org. Chem. Front.*, 2021, **8**, 1117–1124.
22 A. Sarkar, R. Sasmal, C. Empereur-mot, D. Bochicchio, S. V. K. Kompella, K. Sharma, S. Dhiman, B. Sundaram, S. S. Agasti, G. M. Pavan and S. J. George, Self-Sorted, Random, and Block Supramolecular Copolymers via Sequence Controlled, Multicomponent Self-Assembly, *J. Am. Chem. Soc.*, 2020, **142**, 7606–7617.
23 N. Roy, V. Schädler and J.-M. Lehn, Supramolecular Polymers: Inherently Dynamic Materials, *Acc. Chem. Res.*, 2024, **57**, 349–361.
24 S. Y. Dong, B. Zheng, F. Wang and F. Huang, Supramolecular Polymers Constructed from Macrocycle-Based Host–Guest Molecular Recognition Motifs, *Acc. Chem. Res.*, 2014, **47**, 1982–1994.
25 T. Haino, Designer supramolecular polymers with specific molecular recognitions, *Polym. J.*, 2019, **51**, 303–318.

26 A. Harada, Supramolecular Polymers (Host-Guest Interactions), in *Encyclopedia of Polymeric Nanomaterials*, ed. S. Kobayashi and K. Müllen, Springer, Berlin, Heidelberg, 2013, DOI: 10.1007/978-3-642-36199-9_54-1.
27 B. Zheng, F. Wang, S. Dong and F. Huang, Supramolecular polymers constructed by crown ether-based molecular recognition, *Chem. Soc. Rev.*, 2012, **41**, 1621–1636.
28 Z. Duan, F. Xu, X. Huang, Y. Qian, H. Li and W. Tian, Crown Ether-Based Supramolecular Polymers: From Synthesis to Self-Assembly, *Macromol. Rapid Commun.*, 2022, **43**, 2100775.
29 A. Harada, Y. Takashima and H. Yamaguchi, Cyclodextrin-based supramolecular polymers, *Chem. Soc. Rev.*, 2009, **38**, 875–882.
30 U. Schubert, A. Winter and G. Newkome, Supramolecular Polymers, Based on the Host–Guest Chemistry of Calixarenes, in *Supramolecular Polymers and Assemblies*, ed. U. Schubert, A. Winter and G. Newkome, Wiley VCH, 1st edn, 2021.
31 D.-S. Guo and Y. Liu, Calixarene-based supramolecular polymerization in solution, *Chem. Soc. Rev.*, 2012, **41**, 5907–5921.
32 T. Ogoshi, T. A. Yamagishi and Y. Nakamoto, Pillar-Shaped Macrocyclic Hosts Pillar[n]arenes: New Key Players for Supra- molecular Chemistry, *Chem. Rev.*, 2016, **116**, 7937–8002.
33 H. Li, Y. Yang, F. Xu, T. Liang, H. Wen and W. Tian, Pillararene-based supramolecular polymers, *Chem. Commun.*, 2019, **55**, 271–285.
34 T. Kakuta, T. Yamagishi and T. Ogoshi, Stimuli-Responsive Supramolecular Assemblies Constructed from Pillar[*n*]arenes, *Acc. Chem. Res.*, 2018, **51**, 1656–1666.
35 N. Manganaro, I. Pisagatti, A. Notti, M. F. Parisi and G. Gattuso, Self-sorting assembly of a calixarene/crown ether polypseudorotaxane gated by ion-pairing, *New J. Chem.*, 2019, **43**, 7936–7940.
36 N. Manganaro, I. Pisagatti, A. Notti, A. Pappalardo, S. Patanè, N. Micali, V. Villari, M. F. Parisi and G. Gattuso, Ring/Chain Morphology Control in Overall-Neutral, Internally Ion-Paired Supramolecular Polymers, *Chem. – Eur. J.*, 2018, **24**, 1097–1103.
37 C. Capici, Y. Cohen, A. D'Urso, G. Gattuso, A. Notti, A. Pappalardo, S. Pappalardo, M. F. Parisi, R. Purrello, S. Slovak and V. Villari, Anion-Assisted Supramolecular Polymerization: From Achiral AB-Type Monomers to Chiral Assemblies, *Angew. Chem., Int. Ed.*, 2011, **50**, 11956–11961.
38 S. Pappalardo, V. Villari, S. Slovak, Y. Cohen, G. Gattuso, A. Notti, A. Pappalardo, I. Pisagatti and M. F. Parisi, Counterion-Dependent Proton-Driven Self-Assembly of Linear Supramolecular Oligomers Based on Amino-Calix[5]arene Building Blocks, *Chem. – Eur. J.*, 2007, **13**, 8164–8173.
39 A. Notti, I. Pisagatti, F. Nastasi, S. Patanè, M. F. Parisi and G. Gattuso, Stimuli-Responsive Internally Ion-Paired Supramolecular Polymer Based on a Bis-pillar[5]arene Dicarboxylic Acid Monomer, *J. Org. Chem.*, 2021, **86**, 1676–1684.
40 C. Li, S. C. J. Li, K. Han, M. Xu, B. Hu, Y. Yu and X. Jia, Novel neutral guest recognition and interpenetrated complex formation from pillar[5]arenes, *Chem. Commun.*, 2011, **47**, 11294–11296.
41 B. Xia, B. Zheng, C. Han, S. Dong, M. Zhang, B. Hu, Y. Yu and F. Huang, A novel pH-responsive supramolecular polymer constructed by pillar[5]arene-based host–guest interactions, *Polym. Chem.*, 2013, **4**, 2019–2024.
42 J. Chen, H. Ni, Z. Meng, J. Wang, X. Huang, Y. Dong, C. Sun, Y. Zhang, L. Cui, J. Li, X. Jia, Q. Meng and C. Li, Supramolecular trap for catching polyamines in cells as an anti-tumor strategy, *Nat. Commun.*, 2019, **10**, 3546.
43 T. Ogoshi, K. Demachi, K. Kitajima and T. Yamagishi, Monofunctionalized pillar[5]arenes: synthesis and supramolecular structure, *Chem. Commun.*, 2011, **47**, 7164–7166.
44 C. T. Nieto, M. M. Salgado, S. H. Domínguez, D. Díez and N. M. Garrido, Rapid access with diversity to enantiopure flexible PNA monomers following asymmetric orthogonal strategies, *Tetrahedron: Asymmetry*, 2014, **25**, 1046–1060.
45 J. Xu, Y. Chen, L. Wu, C. Tung and Q. Yang, Dynamic Covalent Bond Based on Reversible Photo [4 + 4] Cycloaddition of Anthracene for Construction of Double-Dynamic Polymers, *Org. Lett.*, 2013, **15**, 6148–6151.
46 J. B. Press, W. B. Wright, Jr., P. S. Chan, J. W. Marsico, M. F. Haug, J. Tauber and A. S. Tomcufcik, Thromboxane synthetase inhibitors and antihypertensive agents. 2. *N*-[(1*H*-imidazol-1-yl)alkyl]-1*H*-isoindole-1,3(2*H*)-diones and *N*-[(1*H*-1,2,4-triazol-1-yl)alkyl]-1*H*-isoindole-1,3(2*H*)-diones as unique antihypertensive agents, *J. Med. Chem.*, 1986, **29**, 816–819.
47 A. R. Waldeck, P. W. Kuchel, A. J. Lennon and B. E. Chapman, Prog. NMR diffusion measurements to characterise membrane transport and solute binding, *Nucl. Magn. Reson. Spectrosc.*, 1997, **30**, 39–68.
48 B. A. Jones, M. J. Ahrens, M.-H. Yoon, A. Facchetti, T. J. Marks and M. R. Wasielewski, High–Mobility Air–Stable n–Type Semiconductors with Processing Versatility: Dicyanoperylene–3,4 : 9,10–bis(dicarboximides), *Angew. Chem., Int. Ed.*, 2004, **43**, 6363–6366.
49 N. Pearce, K. E. A. Reynolds, S. Kayal, X. Z. Sun, E. S. Davies, F. Malagreca, C. J. Schürmann, S. Ito, A. Yamano, S. P. Argent, M. W. George and N. R. Champness, Selective photoinduced charge separation in perylenediimide-pillar[5]arene rotaxanes, *Nat. Commun.*, 2022, **13**, 415.
50 I. Pisagatti, D. Crisafulli, A. Pappalardo, G. Trusso Sfrazzetto, A. Notti, F. Nastasi, M. F. Parisi, N. Micali, G. Gattuso and V. Villari, Photoinduced Electron Transfer in Host-Guest Interactions of a Viologen Derivative with a Didansyl-Pillar[5]arene, *Mater. Today Chem.*, 2022, **24**, 100841.
51 F. M. Toma, F. Puntoriero, T. V. Pho, M. La Rosa, Y.-S. Jun, B. J. T. D. Villers, J. Pavlovich, G. D. Stucky, S. Campagna and F. Wudl, Polyimide Dendrimers Containing Multiple Electron Donor–Acceptor Units and Their Unique

Photophysical Properties, *Angew. Chem., Int. Ed.*, 2015, **54**, 6775–6779.

52 D. Rehm and A. Weller, Kinetics of Fluorescence Quenching by Electron and H-Atom Transfer, *Ber. Bunsen-Ges.*, 1969, **73**, 834–839.

53 G. Gattuso, D. Crisafulli, M. Milone, F. Mancuso, I. Pisagatti, A. Notti and M. F. Parisi, Proton transfer mediated recognition of amines by ionizable macrocyclic receptors, *Chem. Commun.*, 2022, **58**, 10743–10756.

54 R. L. Benoit, D. Boulet, L. Séguin and M. Fréchette, Protonation of purines and related compounds in dimethylsulfoxide and water, *Can. J. Chem.*, 1985, **63**, 1228–1232.

55 B. N. Palmer and H. K. J. Powell, Polyamine Complexes with Seven-membered Chelate Rings: Complex Formation of 3-Azaheptane-1,7-diamine, 4-Azaoctane-1,8-diamine (Spermidine), and 4,9-Diazadodecane-1,12-diamine (Spermine) with Copper(II) and Hydrogen Ions in Aqueous Solution, *J. Chem. Soc., Dalton Trans.*, 1974, 2089–2092.

56 B. Barszcz, M. Gabryszewski, J. Kulig and B. Lenatcik, Potentiometric Studies on Complexes of Silver(I) in Solutions. Part 2. Correlation between the Stability of the Silver(I)-Azole Complexes and the Ligand Basicity, *J. Chem. Soc., Dalton Trans.*, 1986, 2025–2028.

57 M. J. Power, D. T. J. Morris, I. J. Vitorica-Yrezabal and D. A. Leigh, Compact Rotaxane Superbases, *J. Am. Chem. Soc.*, 2023, **145**, 8593–8599.

58 Z.-Y. Li, Y. Zhang, C.-W. Zhang, L.-J. Chen, C. Wang, H. Tan, Y. Yu, X. Li and H.-B. Yang, Cross-Linked Supramolecular Polymer Gels Constructed from Discrete Multi-pillar[5]arene Metallacycles and Their Multiple Stimuli-Responsive Behavior, *J. Am. Chem. Soc.*, 2014, **136**, 8577–8589.

59 J. Liu, X. Jiang, X. Huang, L. Zou and Q. Wang, Photo-responsive supramolecular polymer based on a CB[5] analogue, *Colloid Polym. Sci.*, 2016, **294**, 1243–1249.

60 R. Dobrawa, M. Lysetska, P. Ballester, M. Grüne and F. Würthner, Fluorescent Supramolecular Polymers: Metal Directed Self-Assembly of Perylene Bisimide Building Blocks, *Macromolecules*, 2005, **38**, 1315–1325.

61 Y. Yamauchi, K. Yamada, N. N. Horimoto and Y. Ishida, Supramolecular self-assembly of an ABA-Triblock bottle-brush polymer: Atomic-force microscopy visualization of discrete oligomers, *Polymer*, 2017, **120**, 68–72.

62 A. Blacha-Grzechnik, A. Drewniak, K. Z. Walczak, M. Szindler and P. Ledwon, Efficient generation of singlet oxygen by perylene diimide photosensitizers T covalently bound to conjugate polymers, *J. Photochem. Photobiol., A*, 2020, **388**, 112161.

63 S. Winters, C. Backes, N. C. Berner, R. Mishra, K. C. Dumbgen, M. Hegner, A. Hirsch and G. S. Duesberg, On-surface derivatisation of aromatic molecules on graphene: the importance of packing density, *Chem. Commun.*, 2015, **51**, 16778–16781.

64 C. Capici, G. Gattuso, A. Notti, M. Parisi, S. Pappalardo, G. Brancatelli and S. Geremia, Selective Amine Recognition Driven by Host–Guest Proton Transfer and Salt Bridge Formation, *J. Org. Chem.*, 2012, **77**, 9668–9675.

65 G. Brancatelli, G. Gattuso, S. Geremia, A. Notti, S. Pappalardo, M. F. Parisi and I. Pisagatti, Probing the Inner Space of Salt-Bridged Calix[5]arene Capsules, *Org. Lett.*, 2014, **16**, 2354–2357.

66 G. Brancatelli, G. Gattuso, S. Geremia, N. Manganaro, A. Notti, S. Pappalardo, M. F. Parisi and I. Pisagatti, α,ω-Alkanediyldiammonium dications sealed within calix[5]arene capsules with a hydrophobic bayonet-mount fastening, *CrystEngComm*, 2015, **17**, 7915–7921.

67 G. Brancatelli, G. Gattuso, S. Geremia, N. Manganaro, A. Notti, S. Pappalardo, M. F. Parisi and I. Pisagatti, Encapsulation of biogenic polyamines by carboxylcalix[5]arenes: when solid-state design beats recognition in solution, *CrystEngComm*, 2016, **18**, 5012–5016.